Article Type: Research Article

Journal of Neurology and Neurological Sciences

New insights in the pathogenesis and treatment of the unobstructed hydrocephalus: An experimental physical model of the intracranial system

Abstract

The so-called normotensive hydrocephalus is thought to be related to some kind of discrepancy between cerebrospinal fluid production and absorption. Nonetheless, such an explanation is in contrast with further literature data. In order to understand the condition, the authors started to investigate intracranial pulpability as the primary source of ventricular dilatation refining the hypothesis after the introduction of the so-called "Starling resistor". In fact, with its definition, the concept of "asymmetric" response to pulpability started to become the focus of investigation. In order to demonstrate the role of the aforementioned asymmetric response, we created a mechanical model of intracranial circulation in which three different situations were studied, namely normal pulsation, de-pulsation and hyper-pulsation. The experiments were conducted following this scheme: 10 minutes of recording with normal mono sinusoidal pulsation at standard rate, 10 minutes of recording with de-pulsation, 10 minutes of recording with hyper-pulsation, followed by other 10 minutes conducted with bi-sinusoidal pulsation (mimicking carotid pulsation), 10 minutes with de-pulsation, and 10 minutes with hyper-pulsation. In the experiment, the authors could see how during de-pulsation there is an increase of the interstitial volume highlighting the ability of this procedure to treat hydrocephalus. On the contrary, hyper-pulsation does not strictly correlate with the formation of a condition of hydrocephalus, being observed only on 4/6 different situations. Such results could ignite further studies in order to reach a more extensive knowledge on intracranial physiology leading, in the future, to even more tailored kind of therapies.

Federico Bianchi[1]*; Antonio Ficola[4]; Alessandro Rapisarda[2]; Pietro Santini[2]; Francesco Signorelli[2]; Carmelo Anile[3]

[1]Pediatric Neurosurgery, Fondazione Policlinico Universitario Agostino Gemelli IRCCS, Rome, Italy.

[2]Department of Neurosurgery, Fondazione Policlinico Universitario Agostino Gemelli IRCCS, Rome, Italy.

[3]Università Cattolica del Sacro Cuore, Rome, Italy.

[4]Università degli Studi di Perugia, Perugia, Italy.

***Corresponding author: Federico Bianchi**

Pediatric Neurosurgery, Fondazione Policlinico Universitario Agostino Gemelli IRCCS, Rome, Italy.

Email: federico.bianchi@policlinicogemelli.it

Received: May 18, 2026; **Accepted:** Jun 03, 2026; **Published:** Jun 10, 2026

Journal of Neurology and Neurological Sciences

Volume 2 Issue 1 - 2026

www.jnans.org

Citation: Bianchi F, Ficola A, Rapisarda A, Santini P, Signorelli F, et al. New insights in the pathogenesis and treatment of the unobstructed hydrocephalus: An experimental physical model of the intracranial system. J Neurol Neuro Sci. 2026; 2(1): 1027.

Keywords: Hydrocephalus; Model; Pulpability; Starling resistor.

Introduction

Throughout the literature, there are several theories attempting to explain the origin and formation of the so-called normotensive hydrocephalus. Among them, one of the most accredited one theorized some kind of discrepancy between Cerebrospinal Fluid (CSF) production and absorption. Nonetheless, such an explanation is in contrast with further literature data on CSF circulation physiology. In fact, while previous papers highlighted how a reduction in the absorption capacity could lead to hydrocephalus development, they also suggested that the aforementioned decrease was not its cause [1]. Further evidence of the inconsistency of the production/absorption theory resides in the existence of pathologies as intracranial idiopathic hypertension in which it is theorized that a defect in CSF reabsorption capability stand as the pathological mechanism [2]. It is very difficult to conceive that the same issue could act in two opposite ways. More recently, a paper from the European Multicenter Study on INPH (idiopathic) has definitively resolved the question in terms that a defect in the reabsorption capacity may be associated to an increase of ventricular size, but it is not its cause [3].

In the effort to understand such an intricate condition, since the 70s, the authors' institution started to investigate intracranial pulpability as the primary source of ventricular

dilatation [4-7]. However it was only after the definition of the so-called "Starling resistor" [8], that the concept of "asymmetric" response to pulpability started to become the focus of the authors' investigations.

Scientific (Specific) Introduction

In previous papers the author described a model of intracranial system showing how it grant a reliable reproduction of the fundamental mechanisms involved in cerebral circulation [9-11]. Indeed, the physical model (based exclusively on passive components) was able to replicate the mechanisms of the so-called cerebral blood flow autoregulation. In this model, the particularity consists in the role played by the venous outflow, represented by the mechanism known as Starling's resistor [12,13].

In order to comprehend the mechanism leading to a formation of non-obstructive hydrocephalus, we will refer only to the aforementioned part of the total model as a way to show how it resides into a "visible" increase of fluid volume into the ventricular system [9,10]. This concept was defined starting from the simple observation of brain tissue immediate "reappearance" after CSF shunting in normotensive well-treated patients. This evidence led to the hypothesis that movements between the ventricular space and the interstitial or capillary one could be behind such a phenomenon (Figure 1).

To understand the model, it is important to remember that a Starling's resistor is constituted by the region where the bridging veins end connecting firmly themselves at the Dural sinuses. Such a passage is a characterized by a unidirectional valve mechanism in which flow depends both from the difference between intravenous input and output pressure (namely the Vein Pressure [VP]), as well as on the differential pressure between the former and the surrounding spaces (namely the Intracranial Pressure [ICP]). The behavior of this structure in steady condition is well known and was described in previous papers [8,11], but now the authors aim to describe what happens when this mechanism undergoes a periodic, cyclic, pulsatile perturbation as that caused by the arterial expansion in consequence of the cardiac activity.

To explain this new concept, we need to introduce a well-known phenomenon in hydraulic literature [10]. Whenever a fluid passes into a tube that change abruptly its caliber, there is an increase in resistance due to the formation of vortices immediately after the constriction point when the flow runs from more to less caliber and vice versa. In other words, translating this concept into the human physiology, this brusque change in caliber, may introduce an asymmetric behavior following systole, which acts compressing the veins from the external part. On the other hand, during diastole, when the same vessels are forced to be dilated, they tend to remain substantially with a constant caliber. This asymmetric behavior led to a decrease in caliber of a less amount during diastole respect to what increases during systole. At the level of the intracranial compartment, whenever the caliber of the venous vessel changes abruptly it leads to an increase in their resistance thus decreasing flow.

In addition, such effect has also influence onto the interstitial space as its prompt formation and absorption of the fluid in the compartment. In fact, relatively less flow during systole means less fluid formation while relatively more flow during diastole lead to more absorption. Hydrocephalus is then due to a net increase in volume of the fluid within the ventricular space, secondary to fluid displacement from the interstitial space to the ventricles. Such a condition depends from the asymmetrical behavioral of the Starling resistor acting as a pump moving the fluid in and out of the interstitial spaces.

Given the previous explanation, the authors plan to study this condition in the model neutralizing or amplifying intracranial pulsations. In order to do so, the model is implemented with a syringe connected with an electric engine granting the possibility to aspirate the same amount of fluid moved by the arterial pulsation (so decreasing the pulsation) against the walls of the veins (Figure 2, red arrow), or to reintroduce this same amount (so amplifying the pulsation). If our affirmation is correct, we may aspect that during the attenuation of pulsation, the interstitial volume must increase, so indicating the reduction of "hydrocephalus", the opposite condition (hydrocephalus) being simulated by the normal or amplified situation.

The first aim of this paper is then to demonstrate the capability of the reduction of intracranial pulsation as a treatment for ventricular dilation.

Limits

There are some limits to this study; the first one is due to its physic experimental nature; it is impossible, in our experience, to make an analogous experimental condition in a biological environment for the very big difficulties in measuring the same parameters. The second limit is due to the timetable; it is too brief the time scheduled for each experimental situation (10 minutes) to have full cognition of a chronic phenomenon as hydrocephalus is. The third limit is that the increase of intracranial pulsation is of the same shape of the normal wave without those characteristics typical of the waves observed in the hydrocephalic patients [14-16].

Material and methods

We will refer to our previous paper on this model [11] shown in (Figure 2). The physical model is composed of a container that mimics the skull, which encloses the cerebrovascular tree, the ventricular systems and the brain parenchyma. The fluid, which emulates the blood, is supplied by a controlled centrifugal pump, and circulates through arteries, capillaries and veins and goes outside in a reservoir at atmospheric pressure. Two pipes are employed to model the arteries and one of them is connected to the choroid plexus through a shunt. The veins are implemented using two other tubes that split into a certain number of smaller vessels, maximum 10, which mimic the Starling resistor structure.

The interstitial space is replicated by two components, one dynamic (capillary space), made by an aluminum cylinder filled by artificial sponges to simulate the capillary bed, and connected by rigid tubes with the principal cylinder, and one static (interstitial space) made by an easily extensible silastic balloon put within the intracranial system connected by means of a regulable valve to the vascular tree. The difference with the previous experimental condition was the presence with a stopcock connecting the balloon to a syringe graduated in fractions of milliliters so that it was possible after each phase of the experiments to disconnect the balloon from the intracranial circulation and to measure exactly the amount of interstitial fluid contained in its internal volume.

When the basic conditions are well established and non-more changed, we compared what happens to the volume of

the balloon when the system underwent these three different situations: 1) normal pulsation determined by the centrifugal pump; 2) de-pulsation and 3) hyper-pulsation determined by the cyclic aspiration and insufflation od the same amount of fluid from a syringe connected to a control system described in the section named Appendix to Materials and Methods. Each condition is subject to different rate of frequency (standard, 60 beats a minute, slow, 48 beats a minute, and fast, 84 beats a minute) and two different morphology (mono-sinusoidal and like a physiological carotid pulsation made by bi-sinusoidal components).

The experiments were conducted following this scheme: 10 minutes of recording with normal mono sinusoidal pulsation at standard rate, 10 minutes of recording with de-pulsation, 10 minutes of recording with hyper-pulsation, followed by other 10 minutes conducted with bi-sinusoidal pulsation (mimicking carotid pulsation), 10 minutes with de-pulsation, and 10 minutes with hyper-pulsation. This cycle was repeated for standard, slow and rapid rate of frequency.

For each condition, these were the items recorded:

- **IP** - inlet pressure recorded at the entrance of fluid into the total system;
- **DP** - the pressure recorded at the distal part of the tubes mimicking the arterial vascular tree;
- **CP** - capillary or interstitial pressure recorded at the level of the sponge mimicking the capillary or interstitial space and connected to the balloon;
- **VP** - proximal venous pressure recorded at the level of initial part of the tubes mimicking the venous vascular tree;
- **ICP** - intracranial pressure at the level of internal space mimicking the behavior of CSF and cerebral parenchyma;
- **SSP -** sagittal sinus pressure at the extreme late part of vascular tree, after the tubes mimicking the so-called Starling resistor, in the portion open to the atmosphere;
- **IF -** flow of inlet mimicking the carotid flow generated by the pump;
- **OF** - flow of outlet mimicking the sagittal sinus flow.

Six Abbott Transpack® pressure sensors have been inserted to measure the correspondent different pressures. All the signals were also subject to a spectral analysis to measure amplitude and phase of each pressure and flow wave. IF and OF are measured by two GEMS Ft-210® turbine flow rate sensors. A centrifugal submersible pump was chosen to supply about 10-15 cm^3/sec at a pressure of about 100 mmHg. An inverter controls the pump velocity. It is possible to select different velocity profiles and frequencies in the range 48-84 beats/min, as previously said. De-pulsation and hyper-pulsation were obtained by means of the method described in Appendix to this section. Data acquisition is performed by means of a Philips CMS Patient Monitoring System M1167A with a sampling rate 1/128 s. To reduce the measurement noise, signals are post processed using a third order type 2 Chebycheff low-pass filter with 30 Hz cut-off frequency. Signals are filtered forward and backward to prevent phase shift, thus preserving the original wave shape. In addition to this, for all signals the mean value was calculated on 76800 points recorded for each 10 minutes of reported period.

Appendix to materials and methods

The purpose of the control system is to reduce and to increase the pulsatile component of the ICP without affecting its mean value (Figure 3), represent the following control scheme.

ICS is the intracranial system; the intracranial pressure (p_{ic}) is affected by the systemic arterial pressure (Heart) and the syringe driven by an electric motor, whose displacement depends on signal *u*, computed by the control algorithm $R(z)$ in function of the error $e = p_{ic,des} - p_{ic,meas}$ between the desired and measured values of the ICP.

The control algorithm $R(z)$ was developed basing on the following assumptions:

1: ICP is periodic, and the frequency is constant and known (the heart-beat rate) $f = 1/T \equiv \omega/2\pi$

2: A synchronization signal is available (analogue to the QRS signal of the Electrocardiogram);

3: The transfer function between the syringe displacement and the intracranial pressure is minimum phase and fast with respect to the "heartbeat" rate.

According to assumption 1), ICP can be expressed as a Fourier series expansion:

$$p_{ic} = p_{ic\,0} + \sum_{n=1}^{\infty} A_n \sin(n\omega t) + B_n \cos(n\omega t)$$

A pressure transducer measures the ICP, but the signal is corrupted by some noise:

$$p_{ic,sens} = p_{ic} + noise$$

Where noise is assumed Gaussian (non-necessary with zero-mean).

To reject the noise effect, the acquired signal $p_{ic,sens}$ is developed in Fourier series, retaining only the first *N* harmonics, *but the mean value*, thus obtaining the feedback signal:

$$p_{ic,meas} = \sum_{n=1}^{N} a_n(kT)\sin(n\omega t) + b_n(kT)\cos(n\omega t)$$

The coefficients of the Fourier expansion are computed as:

$$a_n(kT) = \frac{1}{T}\int_{(k-1)T}^{kT} p_{ic}(t)\sin(n\omega t)dt \cong \frac{1}{T}\sum_{h=1}^{T/\Delta T} p_{ic}((k-1)T + h\Delta t)\sin(n\omega h\Delta t)$$

$$b_n(kT) = \frac{1}{T}\int_{(k-1)T}^{kT} p_{ic}(t)\cos(n\omega t)dt \cong \frac{1}{T}\sum_{h=1}^{T/\Delta T} p_{ic}((k-1)T + h\Delta t)\cos(n\omega h\Delta t)$$

In our case, the following parameters were considered.

N = 3,

$$\Delta t = \frac{1}{128}s, \quad f = \frac{\omega}{2\pi} = \{48, 64, 80\}bpm \rightarrow T = \frac{1}{f} = \{1.25, 0.9375, 0.75\}s, \quad \omega = \frac{2\pi}{T}rad/s$$

The control signal (namely, the syringe displacement) to be applied for a whole interval T is also periodic:

$$u(k) = \sum_{n=1}^{N} \alpha_n(kT)\sin(n\omega t) + \beta_n(kT)\cos(n\omega t)$$

Where the coefficients α_n, β_n are computed by the control algorithm *R*(*z*) in order to obtain a_n, b_n as small as possible, so that $p_{ic,meas} \approx 0$. A possible algorithm is the following one:

$$\alpha_n((k+1)T) = \alpha_n(kT) + \eta\, a_n(kT), \quad k = 0,1,2,\ldots, \quad \alpha_n(0) = 0$$

$$\beta_n((k+1)T) = \beta_n(kT) + \eta\, b_n(kT), \quad k = 0,1,2,\ldots, \quad \beta_n(0) = 0$$

where η is a gain to be properly chosen? The Z-transforms of A6 with sampling rate *T* are

$$\alpha_n(z) = \frac{\eta}{z-1}a_n(z), \quad \beta_n(z) = \frac{\eta}{z-1}b_n(z)$$

and the regulators are:

$$R(z)=\frac{\eta}{z-1}$$

The integral action is required to get $\alpha_n,\beta_n\neq 0$ even if $a_n,b_n=0$, namely when the control goal $p_{ic,meas}\approx 0$ is achieved.

As far as the stability of the control loop, the open loop function is

$$L(z)=R(z)G(z)$$

where $G(z)$ is the transfer function between the syringe displacement u and the intracranial pressure p_{ic}.

Experiments confirm assumption 3 and show that $G(z)$ is minimum phase, and the dynamics is fast compared with the sampling rate T; therefore, it can be approximated by:

$$G(z)\approx g>0$$

The closed loop function is

$$F(z)=\frac{L(z)}{1+L(z)}\cong\frac{\eta g}{z-(1-\eta g)}$$

Which is asymptotically stable, provided that?

$$|1-\eta g|<1\rightarrow 0<\eta g<2$$

namely if the regulator gain η is sufficiently small.

The control strategy develops in the following stages (Fig. 5). A trigger signal is derived every T seconds (assumption 2); during interval k, $p_{ic,sens}$ is acquired, while control $u(k)$ is applied; at the end of the k-th interval, the values of $a_n(k),b_n(k)$ are computed by means of (A4) and $\alpha_n(k+1),\beta_n(k+1)$ by eqs. (A6); these values determine the control signal $u(k+1)$ to be applied during the subsequent interval k+1.

Because gains α_n,β_n change every T second, control signal $u(k)$ could be discontinuous at instants kT, thus causing transients. The discontinuity effects can be reduced choosing small values of gain η; moreover, they are also smoothed by the dynamics of the electric motor which drives the syringe. Finally, when the control goal is achieved, gains α_n,β_n remain constant and no discontinuity occurs.

Results

The overall results for what concerns the mean values for all the variables considered are: IP oscillates between 96.01 mmHg and 96.55 independently from any kind of the period examined (mono- or bi-sinusoidal, standard, slow, or fast, normal, de-pulsated, or hyper-pulsated); DP from 46.84 mmHg to 47.25 independently from the period examined; CP from 39.59 mmHg to 40.78 mmHg as above; VP from 35.2 mmHg to 35.57 mmHg as above; ICP from 17.93 mmHg to 18.5 mmHg as above; SSP from 17.2 mmHg to 17.8 mmHg as above; IF and OF respectively from 10.61 cm/sec to 11.05 cm/sec independently from the different conditions of the experimental protocol. In summary, the mean values of the different variables were constant during the entire experiment, as expected.

In addition, in the (Figures 4-10), are depicted the differences in volume of the interstitial space in normal, de-pulsation, and hyper-pulsation conditions. It is possible to see how during de-pulsation conditions there is an increase in the volume of interstitial space, indicated by the green up bar, going from 0.1 ml (double slow de-pulsation condition, (Figure 9) to 0.35 ml (double fast, (Figure 10) and finishing to 0.4 (in all the other conditions, (Figures 4-8). During the hyper-pulsation conditions, there is, vice versa, a decrease in the interstitial volume of - 0.4 ml, respect to normal. This happens during mono slow (Figure 5), fast (Figure 6) and double fast (Figure 10) waves, and - 0.3 ml during double slow (Figure 9) waves. On the contrary, in the mono and double standard conditions the authors observed an increase in the amount of fluid in the interstitial space of 0.2 (mono) and 0.6 (double) milliliters (Figures 4 and 8).

For the objectives of this paper, it is very important to look at what happens at level of interstitial or Capillary Pressure (CP), Venous Pressure (VP), Intracranial Pressure (ICP) and Sagittal Sinus Pressure (SSP). We randomly selected and consecutively extracted five waves from a sequence of, respectively, 600, 480 and 840 waves. These are shown in (Figures 4 to 10), during normal, de-pulsation and hyper-pulsation conditions: a clear reduction or amplification in the pulsation of ICP is, as obviously, evident. SSP pressures follow exactly what happens in the ICP. However, the more important data is represented by the behavior of the comparison between CP and VP. Such a behavior appears to pulsate concordantly with ICP and SSP during normal or hyper-pulsation conditions, but it pulsates concordantly with CP during de-pulsation conditions. In other words, the VP seems to precede CP during normal or hyper-pulsation conditions and seems to follow it during de-pulsation conditions. These data are confirmed by the findings shown in (Figure 10), in which is depicted an example of the comparison between CP and VP phases of the fundamental harmonic extracted by six CP and VP simultaneously recorded waves in the three different conditions. These waves are in phase only during de-pulsation conditions and are in opposition of phase in any other conditions.

Moreover, it is of great importance what happens during the simulations conducted with the bi-sinusoidal waves at level of IP; while all the waves assume the same “arterial” configuration, only the CP maintains their uniform mono-sinusoidal shape.

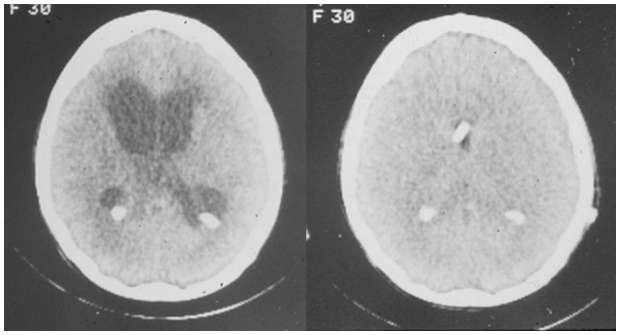

Figure 1: A case of post-traumatic normotensive hydrocephalus before **[A]** and after **[B]** the insertion of an efficacious CSF shunt device; the post-operative picture has been taken few hours after those taken before surgery.

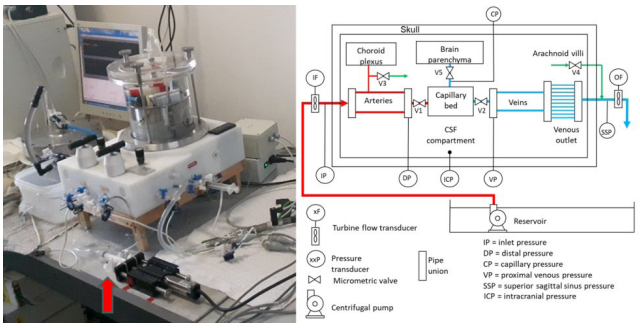

Figure 2: A photogram represents our real experimental condition: the red arrow indicates the syringe working to de-pulsate or hyper-pulsate the ICP.

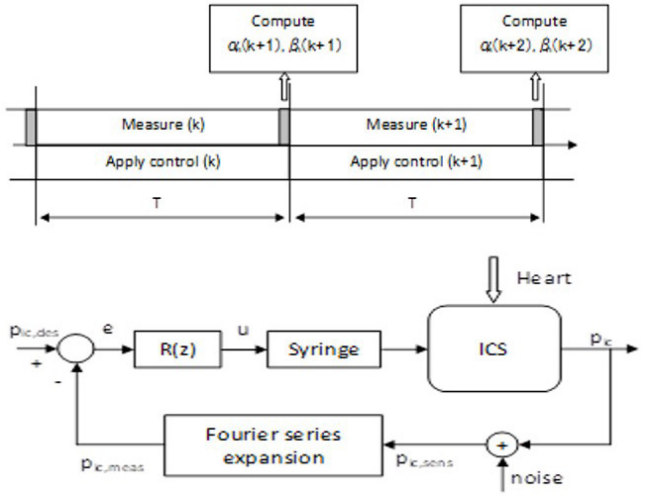

Figure 3: ICP measurement computational methods.

Figure 4: Selection of five consecutive waves randomly extracted by the original recordings. The waves were synchronized with the IP, not shown for clarity and simplicity. They were recorded in a standard condition at 60 beats/minute during normal pulsation **(A)**, during hyper-pulsation **(B)**, and during de-pulsation **(C)**. The graph **(D)** shows the changes in volume of the interstitial space during de-pulsation (green bar) and hyper-pulsation (yellow bar).

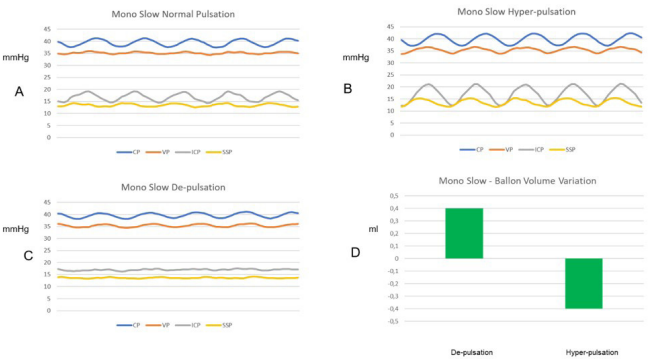

Figure 5: Selection of five consecutive waves randomly extracted by the original recordings. The waves were synchronized with the IP, not shown for clarity and simplicity. They were recorded in a slow condition at 48 beats/minute during normal pulsation **(A)**, during hyper-pulsation **(B)**, and during de-pulsation **(C)**. The graph **(D)** shows the changes in volume of the interstitial space during de-pulsation and hyper-pulsation (green bars).

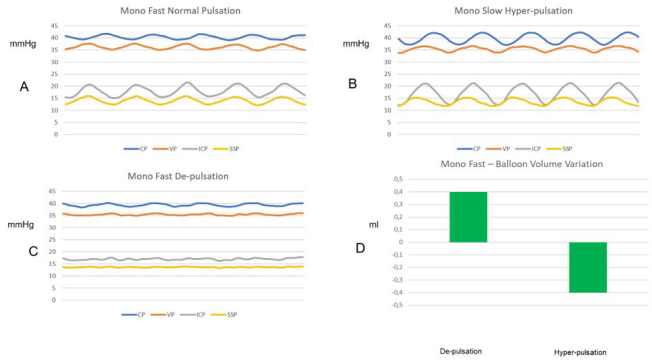

Figure 6: Selection of five consecutive waves randomly extracted by the original recordings. The waves were synchronized with the IP, not shown for clarity and simplicity. They were recorded in a fast condition at 84 beats/minute during normal pulsation **(A)**, during hyper-pulsation **(B)**, and during de-pulsation **(C)**. The graph **(D)** shows the changes in volume of the interstitial space during de-pulsation and hyper-pulsation (green bars).

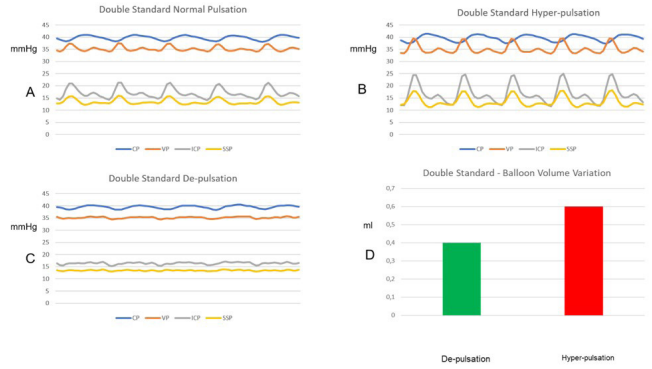

Figure 7: Selection of five consecutive waves randomly extracted by the original recordings. The waves were synchronized with the IP, not shown for clarity and simplicity. They were recorded in a standard condition at 60 beats/minute during normal pulsation **(A)**, during hyper-pulsation **(B)**, and during de-pulsation **(C)**. The graph **(D)** shows the changes in volume of the interstitial space during de-pulsation (green bar) and hyper-pulsation (red bar).

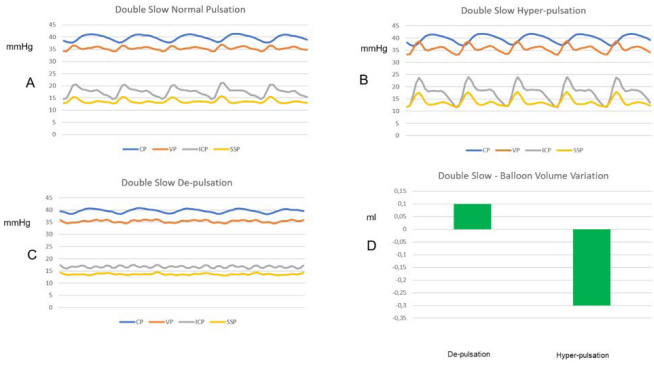

Figure 8: Selection of five consecutive waves randomly extracted by the original recordings. The waves were synchronized with the IP, not shown for clarity and simplicity. They were recorded in a slow condition at 48 beats/minute during normal pulsation **(A)**, during hyper-pulsation **(B)**, and during de-pulsation **(C)**. The graph **(D)** shows the changes in volume of the interstitial space during de-pulsation and hyper-pulsation (green bars).

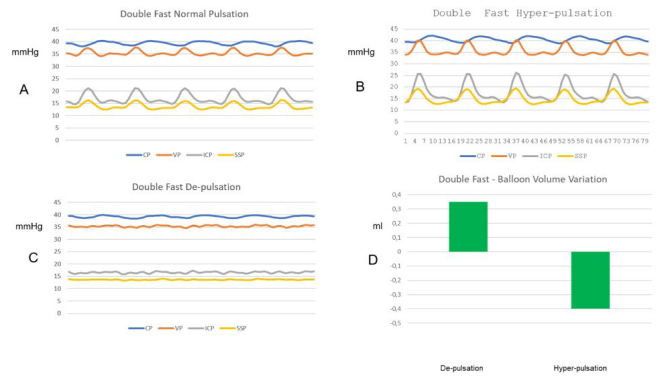

Figure 9: Selection of five consecutive waves randomly extracted by the original recordings. The waves were synchronized with the IP, not shown for clarity and simplicity. They were recorded in a fast condition at 84 beats/minute during normal pulsation **(A)**, during hyper-pulsation **(B)**, and during de-pulsation **(C)**. The graph **(D)** shows the changes in volume of the interstitial space during de-pulsation and hyper-pulsation (green bars).

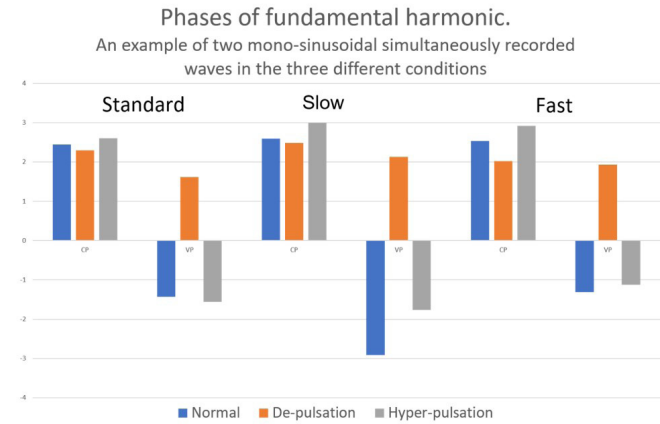

Figure 10: The graph shows the behavior of the phase of the fundamental harmonic of the CP and VP waves in the three conditions of standard, slow and fast pulsation during normal, de-pulsation and hyper-pulsation. These waves are always in an opposition of phase, except during de-pulsation.

Discussion

The first result to be noticed is the absence of any modification in the mean pressure and mean flow of the different variables recorded during the entire duration of the experiment, so signifying the absolute constancy, in terms of mean values, of the different parameters considered, as stated by the experimental conditions.

The second result is the behavior of the amount of the interstitial volume in the three different conditions examined. As expected, the increase of the interstitial volume during de-pulsation condition is direct evidence of the ability of this procedure to treat hydrocephalus. On the contrary, hyper-pulsation does not strictly correlate with the formation of a condition of hydrocephalus, being observed only on 4/6 different situations. This contradictory result may be due to the modality of hyper-pulsation obtained amplifying the normal pulsation [14-16].

In other words, the pulsation coming from the arterial dilation and vehiculated by the CSF on the veins reaches the Starling resistor where the outflow depends mainly by the variable resistance determined by the change in the morphology of this structure: more change means more resistance; less change means less resistance. When the intracranial pressure during the same period of cardiac cycle changes its value from less to more, it determines a less or more changes in the shape of the vein in Starling resistor, but, paradoxically, more change does not signify more flow, but less outflow and less change signify more flow, because of the reduction in parasite resistance.

In a "real" situation, an asymmetrical behavior of the intracranial system is observed. Resistance to fluid circulation is determined by a system of resistances that varies with the shape of the ducts. In this sense, higher resistance values and then lower flows correspond to high-pressure values during systole, whereas lower resistances and then higher flows correspond to low pressure values during diastole. The shape assumed by the bridging veins in their portion entering the upper sagittal sinus, namely the so-called "Starling Resistor", mainly conditions such behavior. During systole, the throttled shape that such vessels assume produces more resistance to the venous outflow than it decreases during the diastolic phase. In this way the production of the interstitial fluid decreases during systole, whereas the absorption of the latter remains unaltered during the diastolic phase, thus inducing, conversely, the formation of hydrocephalus.

This same mechanism may be advocated for what concerns the metabolic aspects: indeed, the permanence of the oxygen in the tissue may be reduced following this mechanism, inducing a relative cyclic chronic state of hypoxia in the brain parenchyma. This consideration may explain the deficit in motor, sphincter, and cognitive functions observed in patients with normotensive hydrocephalus better than other mechanisms based on compressive or stressing forces within an intracranial, closed system in which pressure must be equal in each its part.

Conclusion

Hydrocephalus physiopathology is a very complex mechanism that is still yet to be fully understand. From our experimentation, ventricular enlargement does not seem to be the main issue being changes in interstitial space the major contributor in causing hydrocephalus.

The water in the brain is constant, it is only the distribution of the water which changes, from the brain to the ventricles and vice versa; what regulates this change is the Starling' resistor.

Conflict of interest statement: None.

Acknowledgement: None.

References

1. Børgesen SE, Gjerris F, Sorensen SC. Intracranial pressure and conductance to outflow of cerebrospinal fluid in normal-pressure hydrocephalus. J Neurosurgeon. 1979; 50: 489-93. https://doi.org/10.3171/jns.1979.50.4.0489.

2. Hansen K, Gjerris F, Sorensen PS. Absence of hydrocephalus in spite of impaired cerebrospinal fluid absorption and severe intracranial hypertension. Acta Neurochip (Wien) 1987; 86: 93-7. https://doi.org/10.1007/BF01402291.

3. Vanneste JA. Three decades of normal pressure hydrocephalus: are we wiser now? J Neural Neurosurgeon Psychiatry 1994; 57: 1021-5. https://doi.org/10.1136/jnnp.57.9.1021.

4. Anile C, De Bonis P, Albanese A, Di Chirico A, Mangala A, Petrella G, et al. Selection of patients with idiopathic normal-pressure hydrocephalus for shunt placement: A single-institution experience. J Neurosurgeon 2010; 113: 64-73. https://doi.

org/10.3171/2010.1.JNS091296.

5. Di Rocco C, Maira G, Rossi GF, Vignati A. Cerebrospinal fluid pressure studies in normal pressure hydrocephalus and cerebral atrophy. Eur Neurol. 1976; 14: 1190-28. https://doi.org/10.1159/000114734.

6. Maira G, Di Rocco C, Rossi GF. [Intraventricular pressure in normal pressure hydrocephalus during wakefulness and sleep]. Neurochirurgie. 1974; 20: 462-7.

7. Rossi GF, Maira G, Anile C. Intracranial pressure behaviour and its relation to the outcome of surgical CSF shunting in normotensive hydrocephalus. Neural Res 1987; 9: 183-7. https://doi.org/10.1080/01616412.1987.11739792.

8. Chopp M, Portnoy HD, Branch C. Hydraulic model of the cerebrovascular bed: an aid to understanding the volume-pressure test. Neurosurgery 1983; 13: 5-11. https://doi.org/10.1227/00006123-198307000-00002.

9. Anile C, Ficola A, Santini P. The intracranial system: A new interpretation of the Monro-Kellie doctrine. Arch Anat Physiol. 2021: 001-7.

10. Bansal R. A textbook on Fluid Mechanics and Hydraulic Machines. 9th ed., Laxmi Publications (P) Ltd. New Delhi. 2010.

11. Ficola A, Fravolini L, Anile C. A physical model of the intracranial system for the study of the mechanisms of the cerebral autoregulation. IEEE Access. 2018: 67166-74.

12. Auer LM, Ishiyama N, Hodde KC, Kleinert R, Pucher R. Effect of intracranial pressure on bridging veins in rats. J Neurosurg 1987; 67: 263-8. https://doi.org/10.3171/jns.1987.67.2.0263.

13. Vignes J-R, Dagain A, Guérin J, Liguoro D. A hypothesis of cerebral venous system regulation based on a study of the junction between the cortical bridging veins and the superior sagittal sinus. Laboratory investigation. J Neurosurg 2007; 107: 1205-10. https://doi.org/10.3171/JNS-07/12/1205.

14. Cardoso ER, Rowan JO, Galbraith S. Analysis of the cerebrospinal fluid pulse wave in intracranial pressure. J Neurosurg 1983; 59: 817-21. https://doi.org/10.3171/jns.1983.59.5.0817.

15. Kazimierska A, Kasprowicz M, Czosnyka M, Placek MM, Baledent O, et al. Compliance of the cerebrospinal space: comparison of three methods. Acta Neurochir (Wien) 2021; 163: 1979-89. https://doi.org/10.1007/s00701-021-04834-y.

16. Nucci CG, De Bonis P, Mangiola A, Santini P, Sciandrone M, et al. Intracranial pressure wave morphological classification: automated analysis and clinical validation. Acta Neurochir (Wien) 2016; 158: 581-8; discussion 588. https://doi.org/10.1007/s00701-015-2672-5.